Journal of Environment and Earth Science
ISSN 2224-3216 (Paper) ISSN 2225-0948 (Online)
Vol.16, No.2, 2026

From Rock-Ice Slope Failure to Cascading Flood: The Cryosphere-Geomechanical Destabilization Cascade Model (CGDCM) Applied to the 2026 Nepal-Bhote-Koshi and India-Chamoli 2021 Catastrophes

Gopi Upreti
Emeritus Professor, Tribhuvan University (IAAS), Nepal
Email of the author: goupreti@gmail.com

Abstract
The Bhote Koshi-Trishuli catastrophe in Nepal on August 26, 2026, and the Chamoli disaster in India on February 7, 2021, demonstrate how localized high-mountain glacier rock-ice failures can evolve into catastrophic debris-rich floods through interacting cryospheric, geomechanical, geomorphic, and hydrological processes. This article proposes the Cryosphere-Geomechanical Destabilization Cascade Model (CGDCM), an integrative and testable framework that separates climatic-cryospheric preconditioning from proximate triggering and links progressive weakening, threshold failure, rock-ice detachment, pathway amplification, flow bulking, hydro-geomorphic transformation, societal-infrastructure disruption, and legacy risk. In the model, climatic warming acts primarily by progressively altering glacier support, permafrost integrity, rock-ice bonding, meltwater pathways, and slope stability, rather than by determining the precise moment of failure. Nepal provides strong evidence of impact-generated seismicity, fragmentation, and entrainment-driven amplification along a confined pathway, whereas Chamoli provides complementary evidence of multi-year pre-collapse deformation and water-mediated flow transformation. Recent quantitative reconstruction of the Nepal event provides direct empirical support for the CGDCM distinction between source failure, pathway amplification, and flow transformation. The framework emphasizes that warming may progressively condition slope systems toward instability without necessarily determining the precise moment of failure. Five testable propositions address susceptibility, precursors, pathway amplification, hydrological control of flow regime transitions, and exposure and legacy effects. Operationalization emphasizes measurable physical indicators, rates of change, and site-calibrated multivariate anomaly thresholds rather than universal failure cutoffs. The CGDCM is presented as a bounded, transferable analytical framework whose principal contribution lies in integrating established mechanisms into a coherent source-pathway-river-exposure architecture for analysis, monitoring, and anticipatory Cryospheric Himalayan risk governance.
Key words: Climatic Preconditioning; Rock-Ice Avalanche; Process Chains; Cascading Hazards; Permafrost Thaw; Disaster Risk
DOI: 10.7176/JEES/16-2-06
Publication date: October 28th 2026

1 Introduction

The Hindu Kush Himalaya (HKH), often described as the *Third Pole* and *Water Tower* of Asia, is undergoing rapid cryospheric changes. Glacier thinning and retreat, altered snow persistence, permafrost warming, and changing meltwater pathways modify the thermal, hydrological, and mechanical conditions of steep, high-elevation terrain. Regional assessments and satellite studies have shown accelerating glacier wastage associated predominantly with warming, whereas the Langtang catchment has experienced marked glacier area decline and elevation-dependent warming (Silwal et al., 2026; Azam, 2026; Maharjan and Sherpa, 2026; Upreti, 2023; ICIMOD, 2023; Maurer et al., 2019). These trends establish a changing cryospheric background, but do not identify the immediate trigger of an individual failure.

The August 26, 2026, catastrophe in the Langtang-Lhende-Bhote Koshi-Trishuli system illustrates the difficulty of classifying high mountain catastrophe using a single hazard label. Langtang-Lirung (7,227 m), the highest peak of the Langtang Himal in north-central Nepal, lies near the Nepal–China border in Rasuwa District. The catastrophic ice–rock collapse of 26 August 2026 originated on its steep, glacier-covered northern flank, at approximately 28.2887°N, 85.5282°E (WGS 84), at an elevation of 5,000–5,200 m above sea level. The detached rock–ice mass descended into the upper Lhende Khola catchment, initiating a cascading debris-flow and flood sequence that propagated through the Bhote Koshi–Trishuli river system. A massive rock-ice body

detached near an elevation of 5,200 m, plunged roughly 1,200 m downslope, and generated an earthquake-like seismic signal of 5.4 magnitude through rapid acceleration, violent impact, and fragmentation rather than tectonic shaking. The moving mass then evolved through entrainment, water-sediment interaction, flow transformation, and river-system amplification into a far-reaching debris-rich catastrophic flood (GF, 2026; Richter and Parvaiz, 2026; USGS, 2026).

Event-specific evidence further refines this interpretation. Guo et al. (2026) reconstructed a high-elevation ice-rock avalanche that was progressively amplified by entrainment along an approximately 22-km upper-valley pathway. They found no intense rainfall immediately before failure, identified possible precursor mass transfer signals, and showed that destructive intensity depended strongly on the material acquired during transport. This shifts the analytical attention from the source alone to the evolving source-pathway-river system.

The February 7, 2021, Chamoli disaster in Uttarakhand in India provides a rich data comparison. Approximately 26.9-million-meter^3 of rock and glacier ice detached near Ronti Peak, fell approximately 1,800 m, and transformed into a highly mobile debris-rich flow that devastated the Rishiganga-Dhauliganga valleys (Van Wyk de Vries et al., 2022; Shugar et al., 2021). Subsequent studies have documented multi-year deformation, late-stage acceleration, rock-ice and freeze-thaw mechanisms, water incorporation, entrainment, and flow regime transitions (Li et al., 2025; Wang et al., 2025; Munch et al., 2024; Fan et al., 2022).

1.1 Existing conceptual and modeling approaches to high-mountain cascading hazards

Multi-hazard research provides a broad conceptual foundation for cascading analyses. Kappes et al. (2012) reviewed the methodological challenges in multi-hazard risk assessment, while Gill and Malamud (2014) synthesized interactions among 21 natural hazards and distinguished triggering, intensification, and probability-modifying relationships. Together, these approaches establish the need to analyze interacting hazard sequences rather than isolated hazards.

At the cryosphere-geomechanical scale, Krautblatter et al. (2013) and Mamot et al. (2021) showed how warming, thawing, ice-filled fracture degradation, progressive rock damage, and stress changes can reduce permafrost rock slope stability. Haeberli et al. (2017) linked deglaciation and degrading permafrost to landslides entering newly formed lakes and generating displacement waves or outburst floods, while GAPHAZ (2017) provided operational guidance for glacier-permafrost hazard assessment, monitoring, and risk reduction. At the process-chain scale, Mani et al. (2023) showed how a high-mountain geomorphic process can initiate, transform, or alter subsequent processes. This framework is especially relevant because disaster magnitude may emerge from transformations along the source-to-downstream pathway, rather than from the initial source process alone. Post-detachment dynamics are addressed using multiphase flow models. Pudasaini and Mergili (2019) represented the interaction of coarse solids, fine solids, and fluids, whereas *r.avaflow* simulates complex propagation, entrainment, and flow transformation (Mergili et al., 2025). Alangadan and Sattar (2026) recently coupled permafrost mapping, mass-movement modeling, lake interaction, flood propagation, and downstream exposure in the western Himalaya.

Taken together, these approaches provide a strong foundation for understanding hazard interactions, permafrost and rock slope instability, glacier-related cascades, geomorphic process chains, multiphase flow, and downstream exposure. However, the reviewed literature generally treats these components in separate conceptual and numerical domains. *Therefore, an integrative framework that explicitly links climatic-cryospheric preconditioning, progressive cryosphere-geomechanical weakening, threshold failure, pathway amplification, hydro-geomorphic transformation, downstream exposure, and post-event legacy risk within a single causal architecture is needed.* This research gap motivated the framework developed in Section 3.

Against this background, this study proposes the *Cryosphere-Geomechanical Destabilization Cascade Model (CGDCM)* as an integrative, process-based framework for high-mountain catastrophes initiated by instability in coupled rock-ice-glacier-permafrost terrain. The model is formally presented and described in Section 3, before being applied to the Nepal Bhote Koshi and India's Chamoli cases. The objectives are to: (1) reconstruct the August 2026 Nepal process chain using the strongest available evidence; (2) reconstruct and interpret the 2021 Chamoli event using the same analytical domains; (3) establish the CGDCM architecture and compare it explicitly with antecedent multi-hazard, cryosphere-hazard, process-chain, and multiphase-flow frameworks; (4) evaluate explanatory consistency, transferability, falsifiability, and model boundaries; and (5) derive implications for monitoring, early warning, infrastructure risk assessment, transboundary cooperation, and anticipatory high-mountain risk governance.

2 Methods, Evidence Base, and Case Settings

2.1 Analytical design and literature retrieval

This study used an evidence-based integrative review and comparative process chain analysis rather than a complete forensic field investigation. Nepal evidence prioritizes hydrological reporting from the Department of Hydrology and Meteorology and Flood Forecasting Division; interpretations by the USGS and GFZ; the Science reconstruction of Richter and Parvaiz (2026); and the peer-reviewed study of Guo et al. (2026). Chamoli evidence prioritizes peer-reviewed satellite, seismic, experimental, and numerical studies, including Shugar et al. (2021), Van Wyk de Vries et al. (2022), Fan et al. (2022), Munch et al. (2024), Li et al. (2025), Wang et al. (2025), and Yin et al. (2025).

Targeted literature retrieval used major publisher databases and scientific repositories, including Springer Nature, Wiley, ScienceDirect, Copernicus, Science/AAAS, USGS, GFZ, the Chinese Academy of Sciences, ICIMOD, and Nepalese agency sources, supplemented by backward citation-chaining. Searches combined terms for rock-ice avalanches, Chamoli, Langtang, Bhote Koshi, permafrost rock slopes, glacier de-buttressing, high-mountain process chains, multi-hazard interaction, entrainment, multiphase flow, *r.avaflow*, debris-flow transformation, and cryosphere hazards. Event-specific scientific and institutional evidence available until September 13, 2026, was considered for the rapidly evolving Nepal case. This study is a targeted integrative review and conceptual synthesis rather than a systematic or exhaustive review.

Supplementary regional evidence was also examined to test model boundaries and recurring pathway mechanisms rather than treating every cryosphere-related flood as a direct CGDCM analog. The selected cases included the 1981 Cirenmaco/Zhangzangbo transboundary GLOF, the 2016 Bhote Koshi outburst flood/debris-flow event, the 2024 Thame rock-avalanche-lake displacement cascade, and the July 2025 Lhende-Rasuwagadhi transboundary flood. These cases document contrasting source mechanisms but comparable processes of sediment entrainment, river/lake interaction, transboundary propagation, infrastructure exposure, and post-event reorganization (Stimson Center, 2025, 2026; ICIMOD, 2025; Lamichhane et al., 2021; Liu et al., 2020). They are used as mechanism-level corroboration and boundary tests, rather than as formal validation cases.

Peer-reviewed event reconstructions were given the greatest interpretive weight. Operational agency assessments were used for rapidly evolving observations that were not yet available in the journal literature. Contemporary media reports were retained only when they reproduced technical statements attributable to the named agencies or investigators. Assertions not supported by direct observation, an established physical mechanism, or a traceable technical source were excluded from the causal reconstruction.

2.2 Evidence hierarchy and confidence grading

Two complementary distinctions were used to control causal overstatements. First, the evidence was separated by inferential type. Directly measured or remotely observed information, including rainfall, river stage, flood-wave timing, satellite change, seismic signals, slope displacement, runout, source-volume estimates, and documented impacts, was treated as empirical event evidence. Mechanisms such as glacier de-buttressing, loss of ice-cement strength, freeze-thaw damage, meltwater infiltration, frictional heating, entrainment, flow bulking, and temporary river obstruction were treated as mechanistic interpretations when supported by established literature. Anthropogenic climate change was treated as a long-term conditioning influence on glacier, snow, permafrost, and hydrological boundary conditions; its quantitative contribution to the precise timing of failure was not assumed without formal attribution.

Second, event-specific inferences were graded as having high confidence, moderate confidence, provisional, or unresolved. High confidence was assigned when multiple independent measurements or peer-reviewed reconstructions converged. Moderate confidence was used when a mechanism was physically well supported but incompletely constrained for the event. Provisional was reserved for rapidly emerging interpretations based on limited or newly published evidence. Unresolved indicates competing explanations and insufficient data. Table 1 applies this scheme to principal causal claims.

Table 1 Evidence-confidence matrix for principal event-specific inferences.

Inference	Nepal 2026	Chamoli 2021	Confidence / interpretation
Limited intense antecedent rainfall as primary flood driver	Hydrological reporting and Guo et al. indicate no intense rain immediately before failure.	Not a rainfall-runoff flood; winter event began as rock-ice collapse.	High for excluding a conventional local rainfall-flood explanation in both cases.
Coupled rock-ice source failure	Recent reconstruction estimates an initial ~103 Mm³ rock-ice mass at ~5,190 m a.s.l., including ~12.6 Mm³ of glacier ice (~12%); the exact initiation sequence and source partition remain subject to further verification (Li et al., 2026).	~26.9 million m³ wedge, ~80% rock and ~20% ice.	High for coupled source failure; Nepal now has substantially improved quantitative source constraint, although the exact rock-ice partition and initiation sequence remain provisional.
Progressive pre-failure deformation	Possible precursor tremors/minor mass transfers hours before failure.	>10 m displacement over five years; late-stage acceleration detected.	Chamoli: high. Nepal: provisional.
Cryosphere-geomechanical weakening	Warm-season meltwater, glacier motion and permafrost degradation proposed by new reconstruction.	Permafrost degradation, headwall crack loading, freeze-thaw and rock-ice interaction supported by multiple studies.	Moderate event-specific confidence; strong physical plausibility.
Entrainment-driven pathway amplification	The initial ~103 Mm³ mass descended ~1,180 m and struck/entrained a lower glacier tongue; ~67 Mm³ was deposited in Chhochen Khola and ~36 Mm³ was remobilized into Lende Khola, with progressive entrainment along ~22 km (Li et al., 2026; Guo et al., 2026).	Strong erosion and entrainment during descent; quantified in modelling studies.	High for Nepal, including quantitative evidence of mass redistribution, remobilization, and pathway amplification; moderate-high for Chamoli.
Water-mediated flow transformation	Consistent with melt, sediment and river-water incorporation; quantitative partition unresolved.	Thermomechanical models explicitly reproduce water-sensitive regime transitions.	Nepal: moderate. Chamoli: high.
Temporary river impoundment/breach amplification	Reported in Nepal hydrological reconstruction; detailed geometry still incomplete.	River interaction important, but catastrophic mobility did not depend on a single transient dam-breach sequence.	Nepal: moderate/provisional. Chamoli: event-specific pathway differs.
Anthropogenic climate influence on exact failure timing	Not formally attributed.	Not formally attributed.	Unresolved for precise timing; long-term climate-conditioned susceptibility is well supported regionally.

2.3 Model construction and comparative application procedure

Model construction followed a process chain synthesis, in which observed and literature-supported mechanisms were ordered according to their causal and temporal relationships. The identified domains were climatic-

cryospheric preconditioning, progressive cryosphere-geomechanical weakening, approach to a critical stability threshold, rock-ice or bedrock-glacier detachment, pathway amplification and flow bulking through vertical relief, topographic confinement, entrainment potential, and hydrological availability, flow transformation and hydro-geomorphic coupling, societal-ecological and infrastructure cascade, and legacy-risk landscape. Nonlinear feedbacks among mobility, erosion, entrainment, damming, breach, and renewed amplification were retained, where physically supported. Section 3 describes the resulting model architecture and specifies the procedure used to construct it.

The Nepal Bhote Koshi and India Chamoli events were independently mapped onto the same domains. Similarity was assessed at the process architecture level, not by assuming identical triggers or source composition. Therefore, the comparison tests explanatory consistency and transferability, not formal out-of-sample validation. Chamoli was treated as an independent comparative application that provides strong empirical support for some CGDCM pathways, while the Nepal case provides new evidence for others, especially entrainment-driven pathway amplification.

3 Proposed Cryosphere-Geomechanical Destabilization Cascade Model (CGDCM)

3.1 Conceptual basis and purpose of the CGDCM

The Cryosphere-Geomechanical Destabilization Cascade Model (CGDCM) is proposed as an integrative process-based framework for explaining how long-term climatic and cryospheric change can progressively alter the mechanical stability of coupled rock-ice-glacier-permafrost systems and, following threshold failure, generate cascading geomorphic and hydrological processes whose downstream consequences may greatly exceed the scale of the initial source failure. Therefore, its central analytical unit is not a single hazard type but the evolving source-pathway-river-exposure system. The model distinguishes three causal levels that are often conflated in disaster interpretation: *long-term preconditioning that modifies susceptibility, progressive cryosphere-geomechanical weakening that moves a slope toward instability, and proximate perturbation or internal threshold crossing that determines the final transition to rapid motion.* After detachment, the framework treats relief, confinement, entrainment potential, and hydrological availability as active controls on amplification and flow transformation, rather than as passive properties of the transport corridor.

The CGDCM also distinguishes the physical cascade from disaster and legacy-risk consequences that emerge when the moving mass intersects with exposed people, infrastructure, ecosystems, and an already dynamic river network. This distinction allows the same framework to represent both the mechanics of source-to-downstream transformation and the ways in which exposure, infrastructure interdependence, and post-event landscape reorganization determine the ultimate scale and persistence of the disaster risk. The architecture is presented in Fig. 1 and described stage by stage.

3.2 Model architecture and stage-wise scientific interpretation

Figure 1 presents the CGDCM as two linked domains: *a physical cascade core* that explains the evolution from changing high-mountain boundary conditions to a rapidly transforming mass-flow/flood process, and *a disaster and legacy-risk* extension that explains how the physical cascade interacts with exposure, infrastructure, ecosystems, and the reorganized post-event landscape.

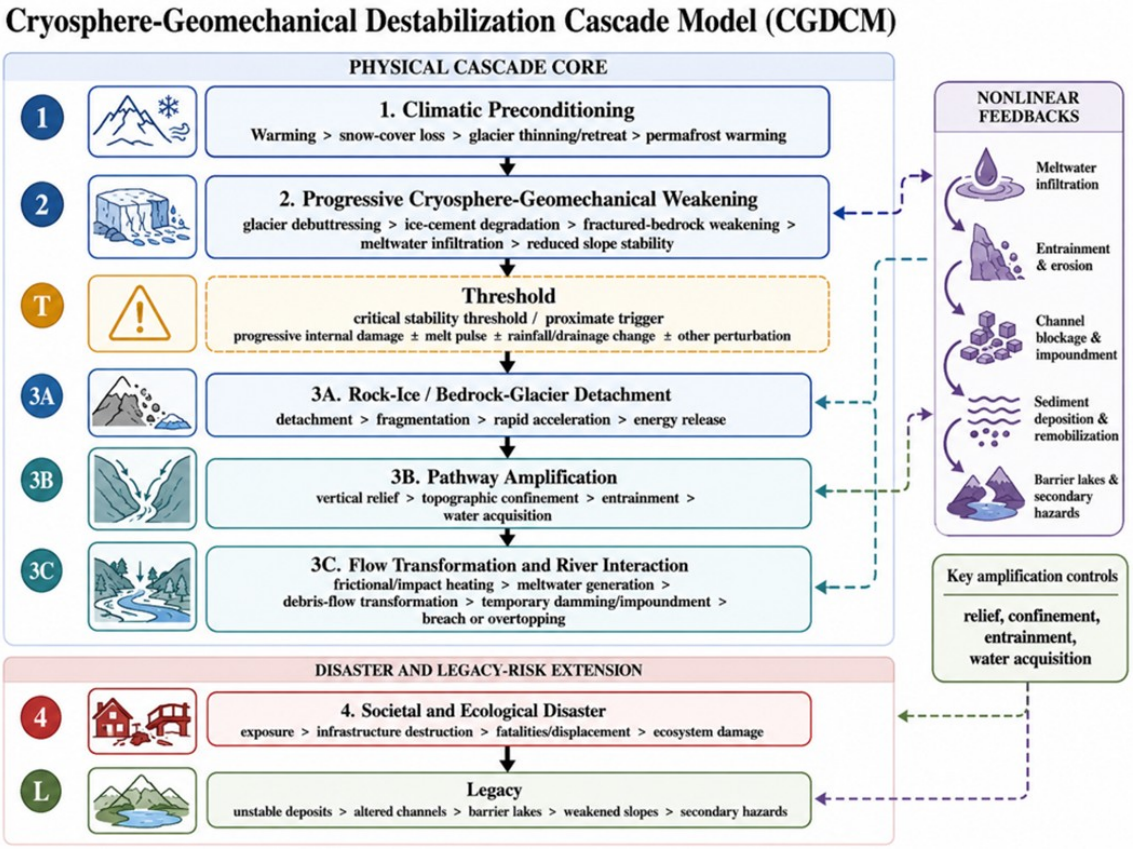


Figure 1. *Cryosphere Geomechanical Destabilization Cascade Model (CGDCM). The physical cascade core comprises climatic-cryospheric preconditioning, progressive cryosphere-geomechanical weakening, critical-threshold crossing, rock-ice/bedrock-glacier detachment, pathway amplification and flow bulking, and flow transformation with hydro-geomorphic coupling. This cascade then intersects with societal, ecological, and infrastructure exposures, producing a legacy-risk landscape. Nonlinear feedback may renew or amplify the later stages.*

Stage 1: Climatic-cryospheric preconditioning. The model begins with the long-term modification of the high mountain environment rather than the catastrophic event itself. Atmospheric warming, changes in snow cover persistence, glacier thinning and retreat, permafrost warming, and meltwater/drainage reorganization alter thermal, hydrological, and mechanical boundary conditions. This stage represents susceptibility enhancement, not the direct attribution of individual failure. A warmer cryosphere may shift a slope closer to instability without determining the precise day or hour of failure.

Climatic preconditioning should be understood as a *cumulative destabilization* process, rather than a discrete trigger. Sustained atmospheric warming progressively modifies the cryospheric and geomechanical boundary conditions of high-mountain slopes through glacier thinning and retreat, loss of buttressing support, permafrost warming and thawing, intensified freeze-thaw cycling, increased meltwater production, and reorganization of surface and subsurface drainage. These changes can weaken rock-ice bonds, enlarge fractures, promote meltwater infiltration and pore pressure development, redistribute stresses, and progressively reduce the mechanical resistance of coupled rock-ice-glacier systems. Over time, an initially stable slope may evolve toward a metastable or near-critical condition in which increasingly small perturbations or continued internal deterioration alone may be sufficient to cross the failure threshold. In the CGDCM, climatic forcing primarily acts by progressively conditioning the mountain system toward instability rather than by determining the precise moment of failure. Therefore, climate change may load the mountain system with instability without necessarily pulling the final trigger.

Stage 2: Progressive cryosphere-geomechanical weakening. Changing cryospheric conditions are translated into mechanical instability through glacier debuttressing, degradation of rock-ice bonds and ice-cemented fractures, fracture propagation, meltwater infiltration into the cracks and crevices of the rock, pore-pressure changes, and stress redistribution. Therefore, the coupled glacier-permafrost-bedrock system may progressively lose its resistance. This domain is central to the CGDCM because it provides a physical bridge between regional climate change and eventual threshold failure.

The Langtang glacier reconstruction of Silwal et al. (2026) provides a regionally relevant illustration of how long-term climatic preconditioning may translate into changing mechanical boundary conditions. Accelerated glacier thinning, fragmentation, and disconnection can modify glacier geometry and support conditions, while rising equilibrium-line altitudes and thinning in steep icefall zones indicate sustained cryospheric reorganization. These changes may interact with permafrost degradation, weakening of ice-filled rock fractures, and meltwater-mediated changes in effective resistance. Glacier recession is therefore not merely an indicator of climatic change: on susceptible slopes, it may contribute to progressive changes in mechanical stability. CGDCM represents this intermediate transition between climatic forcing and critical-threshold failure.

Critical stability threshold and proximate perturbations. The threshold is the transition from a progressively weakened but metastable slope to a rapid failure. The model is deliberately trigger-agnostic. Threshold crossing may follow internal damage accumulation alone or may be assisted by a short thermal or melt pulse, rapid drainage change, rainfall, snow loading, seismic shaking, or other perturbations. In some events, the final perturbation may never be identified unambiguously. Distinguishing the long-term preconditioned state from proximate perturbations prevents causal overstatements.

Stage 3A - Rock-ice/bedrock-glacier detachment. Once the resistance falls below the forces driving the motion, a part of the coupled slope system detaches. Gravitational potential energy is rapidly converted into kinetic energy, resulting in acceleration, impact, fragmentation, and intense comminution. Depending on the source geometry, the failed mass may be rock-dominated, ice-dominated, or a mixed rock-ice body. Therefore, the CGDCM does not require a single source composition; it requires a coupled high-mountain failure capable of initiating a downstream cascade.

Stage 3B: Pathway amplification and flow bulking. The transport corridor is treated as an active component of hazard generation, not merely as a route between the source and receptor. Vertical relief supplies energy, topographic confinement sustains flow concentration, entrainment potential determines how much additional rock, sediment, snow, ice, vegetation, and channel material can be incorporated, and hydrological availability controls the amount of water acquired from melting, wet sediment, rivers, subsurface flow, and transient lakes. Consequently, the moving mass can increase substantially in terms of volume, momentum, and mobility after source failure.

Stage 3C: Flow transformation and hydro-geomorphic coupling. Fragmentation, frictional and impact heating, ice/snow melt, water-sediment mixing, and external water incorporation can transform a rock-ice avalanche into a debris flow, debris flood, or hyper-concentrated flood. Interactions with rivers or lakes may create additional amplification through temporary damming, displacement waves, overtopping, breaches, channel erosion, or rapid release of stored water and sediment. These mechanisms are conditional rather than obligatory, and different events may activate different pathways within the same CGDCM architecture.

Stage 4: Societal-ecological and infrastructure cascade. Physical hazards become catastrophic disasters when they intersect with exposed people, settlements, hydropower facilities, roads, bridges, border infrastructure, communication systems, and ecosystems. The failure of one infrastructure component may then propagate through other systems: bridge loss can isolate communities, road failure can obstruct rescue, power loss can disrupt communication, and hydropower damage can affect regional energy supply. Therefore, the model distinguishes physical cascade amplification from the additional amplification created by exposure and systemic vulnerability.

Legacy-risk landscape. The cascade does not end when the principal flood wave passes. Large sediment stores, altered channels and drainage, new barrier lakes, weakened slopes, and damaged infrastructure establish a new post-event-hazard baseline. Secondary remobilization, renewed damming or breach, and subsequent slope failure can generate additional hazards for months to years. Therefore, the CGDCM treats catastrophe as a landscape transition that resets future risks rather than an isolated terminal event.

Nonlinear feedbacks. Feedback connects the stages and can magnify the cascade: greater mobility increases erosion; erosion increases entrainment; entrainment increases mass and momentum; increased debris can promote damming; damming can store water; breach can create renewed amplification; and the resulting deposits can reorganize later flow paths. These feedbacks explain why downstream intensity may be disproportionate to the initial source volume and why static single-hazard models can underestimate complex high mountain risk.

3.3 Relationship of the CGDCM to antecedent frameworks

Once the CGDCM architecture is made explicit, its relationship with earlier frameworks can be assessed more precisely. The CGDCM builds upon, rather than replaces, established multi-hazard, cryosphere-hazard, geomorphic process chain, and multiphase-flow science. The broad multi-hazard approaches of Kappes et al. (2012) and Gill and Malamud (2014) establish that hazards interact and can trigger, intensify, or modify subsequent processes; the CGDCM places this general interaction logic within a cryosphere-specific source-to-downstream causal sequence.

The temperature-dependent rock-slope models of Krautblatter et al. (2013) and Mamot et al. (2021) provide direct mechanistic foundations for progressive cryosphere-geomechanical weakening, whereas Haeberli et al. (2017) and GAPHAZ (2017) demonstrate how deglaciation, permafrost degradation, slope failure, lake interaction, scenario assessment, and monitoring can be linked to changes in mountain terrain. Mani et al. (2023) provide the closest conceptual antecedent at the process-chain level by showing that high mountain hazards evolve through linked transformations rather than isolated events.

In the post-detachment stage, the multiphase formulation of Pudasaini and Mergili (2019) and the r.avaflow framework of Mergili et al. (2025) provide the physical and numerical foundations for entrainment, material interaction, water incorporation, and flow transformation. Alangadan and Sattar (2026) extended this systems perspective through a Himalayan multi-model architecture linking permafrost degradation, mass movement, lake interaction, flood propagation, and downstream exposure. These approaches overlap with different portions of the CGDCM, but do not, in the literature reviewed here, combine all of its pre-failure, pathway-amplification, hydro-geomorphic, societal, and legacy-risk domains within one bounded framework.

Table 2 summarizes this lineage. The comparison is intentionally made after the CGDCM has been defined and described so that similarities and differences are evaluated against a clearly specified model rather than anticipated before the reader has seen the proposed architecture.

Table 2 Relationship of the CGDCM to established multi-hazard, cryosphere-hazard, process-chain, and multiphase-flow frameworks.

Framework / model	Primary focus	Relationship with CGDCM	CGDCM integration / extension
Multi-Hazard Risk Analysis Framework (Kappes et al., 2012)	Multi-hazard risk analysis and comparability across hazards.	General foundation for an integrated hazard analysis.	It adds cryosphere-specific causal staging and process amplification.
Natural Hazard Interaction Framework (Gill and Malamud, 2014)	Interaction networks in which one hazard triggers or increases the probability of another hazard.	Supports cascading and nonlinear hazard interaction logic.	Adds detailed high-mountain source, pathway, hydro-geomorphic and legacy domains.
Permafrost Rock-Slope Destabilization Models (Krautblatter et al., 2013; Mamot et al., 2021)	Temperature-dependent weakening and stability of permafrost-rock slopes.	Mechanistic foundation for progressive cryosphere-geomechanical weakening.	Weakening is extended through threshold failure, runout transformation, exposure, and legacy risk.
Deglaciation-Permafrost-Landslide-Lake Cascade Framework (Haeberli et al., 2017)	Deglaciation/permafrost degradation -> landslide into new lake -> displacement wave/outburst wave.	Close hydro-geomorphic cascade analog.	Accommodates lake-mediated and direct rock-ice-to-debris-flood pathways.
Glacier and Permafrost Hazard Assessment Framework - GAPHAZ (GAPHAZ, 2017)	Glacier/permafrost hazard assessment, scenarios, monitoring and risk reduction.	Operational and assessment foundations.	Link monitoring and management to an explicit causal cascade architecture.
High-Mountain Geomorphic Process-Chain Framework (Mani et al., 2023)	High-mountain geomorphic process chains and transformations.	Closest conceptual antecedent.	Explicitly adds cryosphere-geomechanical weakening, trigger separation, societal/infrastructure cascades, and legacy risks.
Multiphase Mass-Flow / r.avaflow Modeling Framework (Pudasaini and Mergili, 2019; Mergili et al., 2025)	Multiphase mass-flow physics and numerical propagation of complex landslides.	Physical/computational basis for Stages 3 B–3 C.	It adds climatic preconditioning, threshold mechanics, exposure, and post-event risk.
Permafrost-Mass Movement-GLOF Multi-Model Architecture (Alangadan and Sattar, 2026)	Permafrost mapping linked to modeled mass movement, lake interaction, flood propagation, and exposure.	The closest recent Himalayan modeling analog to part of the CGDCM.	Broader bounded architecture for coupled rock-ice initiation, pathway amplification, direct river coupling, and legacy risk.

3.4 Scientific novelty, scope, and model boundaries

The scientific contribution of the CGDCM lies not in claiming novelty for individual processes, such as glacier retreat, permafrost degradation, rock slope failure, entrainment, debris-flow transformation, river interaction, or infrastructure exposure, all of which have substantial precedent. Its proposed novelty is synthetic and architectural: it explicitly separates climatic-cryospheric preconditioning from progressive cryosphere-geomechanical weakening and proximate threshold crossing; treats the transport pathway as an active amplification system; incorporates hydro-geomorphic transformation and nonlinear feedbacks; and extends the physical cascade into societal-infrastructure consequences and a post-event legacy-risk landscape.

The CGDCM is primarily intended for high-mountain cascades initiated by instability in coupled rock-ice-glacier-permafrost terrain. It is not proposed as a universal model for every glacial lake outburst flood, rainfall-induced debris flow, or tectonically triggered landslide. Such events may intersect the framework at the downstream transformation, river interaction, exposure, or legacy-risk stages, but they do not necessarily share their cryosphere-geomechanical source pathway. This bounded but flexible scope preserves explanatory discipline while allowing comparative application across a wider range of high-mountain cascading events. To clarify transferability, the framework distinguishes three levels of generalization: the overall process architecture is transferable; the activation, ordering, and relative importance of individual pathways are event-specific; and numerical warning thresholds are site-specific and require local calibration. This distinction permits comparative use without assuming that different mountain systems share identical triggers, source compositions, or critical values.

The model is a structured hypothesis system rather than a deterministic sequence in which every process must occur. Individual stages can be supported, rejected, or modified as higher resolution data become available. Nepal 2026 and Chamoli 2021 are therefore treated as comparative applications and consistency tests, not as formal out-of-sample validations. The Results section examines how the evidence from each case maps onto the defined model domains, where the two events diverge and where uncertainty remains.

4 Results

4.1 August 2026 Bhote Koshi-Trishuli catastrophe, Nepal

4.1.1 Hydrometeorological and hydrological reconstruction

The flood hydrograph indicates an abrupt high-altitude input rather than a progressive local catchment runoff. At approximately 08:40 Nepal time, the Bhote Koshi-Syafrubesi hydrological station recorded a stage of approximately 1.62 m, far below its 6 m warning level and 7 m danger level. Transmission ceased around 08:50, and by approximately 09:00, authorities had information that an exceptional surge was entering the Bhote Koshi system from the transboundary headwaters. The Betrawati station ceased transmission at approximately 09:20. The flood reached Galchhi at approximately 10:28, Malekhu around 11:50, Muglin around 13:00, and Devghat around 15:20; the Devghat stage peaked near 6.57 m at about 16:00. Four automatic hydrological stations were destroyed, and Nepal's Flood Forecasting Division estimated that approximately 20-million-meter ^{3} of additional floodwater passed through Devghat during the event (OnlineKhabar, 2026b).

This extreme downstream response occurred despite the limited local rainfall in Rasuwa. Nepalese hydrometeorological reporting indicated only approximately 7 mm during the preceding 24 h, whereas Guo et al. (2026) reported below-average precipitation in the source region during the preceding months and no intense rainfall immediately before the failure. Rainfall or antecedent moisture may have influenced the local slope or sediment conditions, but the evidence is inconsistent with a conventional local rainfall-runoff explanation for the magnitude of the flood (Guo et al., 2026; OnlineKhabar, 2026a).

4.1.2 Source failure, precursor signals, and uncertainty

Source interpretation evolved as higher-resolution imagery and seismic analyses became available. Richter and Parvaiz (2026) reported that investigators increasingly favored landslides involving glacier ice rather than autonomous glacier collapses. Subsequent seismic interpretation indicated that the earthquake-like signal was produced by the mass movement itself rather than by a tectonic earthquake: a massive rock-ice body detached at approximately 5,200 m elevation, plunged roughly 1,200 m downslope, and generated intense seismic energy via rapid acceleration, violent impact, and fragmentation. GFZ estimated flow velocities of approximately 40-50 m/s, while USGS classified the event more conservatively as rapid slope failure involving a glacier, reported

debris-flow/flood runout of roughly 100 km, and estimated the generated seismic energy as equivalent to an earthquake of approximately magnitude 5.2 (GFZ German Research Centre for Geosciences, 2026; U.S. Geological Survey, 2026). ICIMOD's rapid event assessment likewise characterized the disaster as a Nepal-China cryosphere-risk cascade involving high-altitude ice, rock, sediment, and downstream river interaction (International Center for Integrated Mountain Development, 2026b).

Guo et al. (2026) added a complementary peer-reviewed reconstruction centered on a massive high-elevation ice-rock avalanche on the northern slope of Langtang Lirung. This study links source susceptibility to long-term glacier motion, unusually warm spring-summer conditions that increase meltwater availability, and high-altitude permafrost degradation, while finding no evidence of a single short-term rainstorm trigger. Seismic stations also recorded several anomalous tremors in the hours before the principal event, some corresponding to reported minor snow or ice activity. These signals suggest possible precursor mass transfer, but their predictive significance remains provisional. A recent high-resolution reconstruction provides substantially stronger quantitative constraint on the initial failure and its early transformation. Li et al. (2026), integrating remote-sensing, seismological, hydrological, field, and numerical evidence, estimated that an approximately 0.76 km² rock-ice mass with a total volume of ~103 Mm³ failed from the north flank of Langtang Lirung at approximately 5,190 m a.s.l., including about 12.6 Mm³ of glacier ice (~12%). After roughly 30 s of descent, the mass struck and entrained a detached glacier tongue near 4,010 m a.s.l., corresponding to an initial vertical descent of approximately 1,180 m, and rapidly evolved into a large rock-ice avalanche. Within the following ~100 s, approximately 67 Mm³ of debris was deposited in Chhochen Khola, whereas the remaining ~36 Mm³ was remobilized as a highly mobile debris flow that entered Lende Khola (Li et al., 2026).

For the 2026 Nepal catastrophe, the available evidence is therefore more appropriately interpreted in terms of climatic preconditioning than direct single-event climate causation. Long-term warming, glacier thinning and retreat, possible degradation of permafrost and ice-filled fractures, enhanced seasonal melting, and changing freeze-thaw conditions may have progressively reduced the stability of the coupled rock-ice slope system (Guo et al., 2026; ICIMOD, 2026a; Silwal et al., 2026). Such processes would not necessarily determine the exact timing of collapse, but they could increase the probability that the slope approaches a critical stability threshold. Therefore, the relevant question is not simply whether climate change triggered the August 26 failure, but whether anthropogenic warming altered the physical boundary conditions sufficiently to increase the probability of destabilization.

The combined evidence supports a coupled high-elevation rock-ice slope failure with high confidence; however, the precise initial partition between bedrock detachment and glacier failure remains unresolved. Bedrock involvement is strongly plausible from the Science, GFZ, and USGS reconstructions, whereas the Science Bulletin study emphasizes ice-rock avalanche dynamics and glacier instability. Therefore, the CGDCM avoids forcing the event into a single categorical source label and instead treats bedrock, ice, permafrost, meltwater, and gravitational stress as interacting components of a coupled slope system. Although the precise source composition remains subject to further independent verification, Li et al. (2026) estimate approximately 12.6 Mm³ of glacier ice, equivalent to about 12% of the ~103 Mm³ initial failed mass. This event-specific estimate provides substantially improved quantitative constraint but should not yet be interpreted as a universal or definitive partition of the coupled bedrock-glacier failure. No definitive bedrock-to-ice ratio is therefore assigned for the Nepal event; any current numerical source partition should be regarded as provisional until high-resolution volume reconstruction, field evidence, and additional remote-sensing analyses provide stronger constraint.

Long-term glaciological observations provide additional context for evaluating source-region susceptibility. Silwal et al. (2026) documented fragmentation of Lirung Glacier and earlier disconnection of its debris-covered lower tongue from the upper glacier. Such geomorphic reorganization is relevant to possible changes in glacier support, mechanical connectivity, and stability at steep rock–ice interfaces. However, establishing whether these documented changes directly affected the specific detachment surface involved in the 26 August 2026 event requires precise spatial correlation and event-specific geomechanical evidence.

4.1.3 Pathway amplification, flow transformation, and river interaction

These quantitative mass-balance estimates provide direct empirical support for the CGDCM distinction among initial detachment, pathway amplification, and flow transformation. The reconstructed Nepal source volume (~103 Mm³) is substantially larger than the ~26.9 Mm³ rock-ice wedge documented for Chamoli 2021, although direct volume comparison should be interpreted cautiously because source compositions and reconstruction methods differ (Shugar et al., 2021; Van Wyk de Vries et al., 2022). More importantly, the ~36 Mm³ value for

Nepal represents the remobilized downstream component after major deposition, not the initial source volume. The observed redistribution from an initial ~103 Mm³ failure to ~67 Mm³ of deposition and ~36 Mm³ of remobilized debris demonstrates that downstream hazard cannot be inferred from source volume alone; mass redistribution, glacier impact and entrainment, water incorporation, topographic confinement, and flow-regime transformation govern the evolving destructive potential of the cascade (Li et al., 2026). The strongest new process chain evidence concerns progressive entrainment. Guo et al. (2026) concluded that the final destructive intensity was not determined by the initial source volume alone. During descent through the steep, confined gully, the moving mass scoured the channel beds and margins and incorporated loose rock, moraine, sediment, snow, ice, soil, vegetation, and water. Therefore, the transport path became an active source of additional mass and momentum. This directly supports the CGDCM concept that vertical relief supplies gravitational energy, confinement maintains flow concentration, and entrainment-driven bulking can nonlinearly enlarge the moving mass during propagation.

Fragmentation, collision, frictional and impact heating, ice melt, and mixing with river water promoted the transformation from a rock-ice avalanche into a water-rich debris flow or debris flood. Nepal's hydrological reconstruction also indicates temporary obstruction or impoundment within the river system, followed by release, providing a further mechanism for flood-wave amplification (OnlineKhabar, 2026b). Therefore, the downstream hazard was not simply the original source mass translated downslope; it was a dynamically evolving multiphase flow whose volume, water content, density, momentum, and peak discharge changed through interactions with the transport corridor and river network. The relative contributions of frictional or impact melt, wet sediment, subsurface water, and river water have not yet been quantitatively partitioned. Likewise, the geometry, duration, impounded volume, and breach dynamics of any temporary channel obstruction remain incompletely constrained. Accordingly, water-volume partitioning and impoundment/breach amplification are treated here as provisional event-specific pathways rather than fixed components of the Nepal reconstruction.

4.2 The 2021 Chamoli disaster, Indian Himalaya

4.2.1 Pre-collapse deformation and threshold failure

On February 7, 2021, approximately 26.9-million-meter³ of rock and glacier ice detached from the steep north face of Ronti Peak, dropped approximately 1,800 m to the Ronti Gad valley floor, and propagated into the Rishiganga and Dhauliganga valleys. The failed wedge was approximately 80% bedrock and 20% glacier ice (Shugar et al., 2022; Shugar et al., 2021). Therefore, the event was not a glacial lake outburst but a rock-ice slope failure that subsequently transformed into a destructive debris-rich flow.

Chamoli provides unusually strong evidence of progressive pre-failure instability. Feature tracking and digital elevation models showed that the eventual failure block moved more than 10 m horizontally and vertically during the five years preceding the collapse, with particularly rapid motion in the summers of 2017 and 2018 (Van Wyk de Vries et al., 2022). Independent multi-temporal satellite analysis identified late-stage acceleration with maximum deformation velocities of approximately 0.5 m/day in the days before collapse (Fan et al., 2022). These observations provide strong empirical support for the CGDCM proposition that catastrophic detachment represents the terminal stage of progressive geomechanical weakening.

However, the exact threshold-crossing mechanism remains unclear. Van Wyk de Vries et al. (2022) proposed a combination of snow loading in a deep headwall crack and permafrost degradation in heavily jointed bedrock. Zhou et al. (2021) emphasized the combined effects of climate and weather. More recent experiments indicate that freeze-thaw cycling, pore-water pressure fluctuations, meltwater infiltration, and progressive loss of rock-ice interfacial strength can promote instability (Li et al., 2025). Coupled DDA-SPH simulations further show that temperature-dependent glacier creep can alter the stress concentration and fracture propagation in the underlying rock (Wang et al., 2025). These findings strengthen the plausibility of coupled cryosphere-geomechanical weakening but do not reduce failure to a single climatic trigger.

4.2.2 Flow transformation, entrainment, and secondary hazards

Once detached, the extreme relief converted the gravitational potential energy rapidly into kinetic energy. The impact on the valley floor generated fragmentation, a large powder cloud, erosion, and progressive entrainment. The moving mass incorporated river sediment, older deposits, snow, and water as it propagated through Ronti Gad. Shugar et al. (2021) documented the transformation of the initial rock-ice avalanche into an exceptionally mobile debris flow that transported very large boulders, scoured valley walls, and severely damaged downstream hydropower infrastructure.

Thermomechanical modeling has further refined this mechanism. Munch et al. (2024) represented an avalanche as interacting rock, ice, snow, and water phases and explicitly modelled frictional heating, phase change, ground entrainment, and flow regime transition. Their results showed that water is a critical control on mobility, but the water source cannot be reduced to frictional melting of glacier ice alone; wet sediment, river water, and subsurface water entrained along the pathway can make major contributions. Relatively small changes in water content can shift the moving mass from granular or debris-flow behavior to a more mobile hyper-concentrated flood regime.

Recent studies have reinforced the importance of pathway evolution. Gao et al. (2026), analyzing the 2018 Sedongpu rock-ice avalanche-debris-flow cascade in southeastern Tibet, found that saturated moraine entrainment could drive a rapid transition from avalanche to water-rich debris flow, independently supporting the CGDCM emphasis on external water and substrate entrainment. Chamoli also generated branching hazards: numerical reconstruction indicates avalanche-induced air blasts exceeding 70 m/s and 20 kPa in parts of the Ronti Gad Valley (Yin et al., 2025). These branching effects demonstrate that pathway amplification can generate multiple interacting hazards rather than a single linear downstream process.

4.3 Comparative process architecture

The two disasters differed in terms of source geometry, evidentiary maturity, and hydrological context. Chamoli has a well-constrained source volume and composition and a multi-year deformation record, whereas the Nepal source mechanism is still being refined. Nepal propagated through a transboundary river system over a much longer downstream reach and provided direct evidence that progressive entrainment over the first approximately 22 km controlled the final intensity. By contrast, Chamoli offers stronger evidence for pre-collapse slope motion and a more mature thermomechanical simulation of flow regime transformation.

Despite these differences, both events share a higher-order architecture: a cryosphere-modified steep rock-ice system evolves toward instability; threshold failure releases a high-energy mixed mass; relief and confinement accelerate the flow; fragmentation, entrainment, melt, and external hydrological availability change the moving mixture; valley and river interactions amplify mobility and spatial reach; and concentrated downstream exposure converts the physical cascade into a catastrophe. Table 3 maps both cases onto the same CGDCM domains while preserving the differences in confidence and mechanism.

Table 3 Comparative application of the CGDCM to Nepal 2026 and Chamoli 2021.

CGDCM domain	Nepal 2026	Chamoli 2021	Comparative interpretation
1. Climatic-cryospheric preconditioning	Rapidly changing Langtang cryosphere; warm spring-summer conditions, meltwater and possible permafrost degradation.	Regional warming, permafrost degradation, snow/ice loading and glacier-rock interaction proposed.	Supports susceptibility context, not direct single-event attribution.
2. Cryosphere-geomechanical weakening	Coupled rock-ice instability; possible short-term precursor mass transfers.	Multi-year deformation, deep headwall crack, jointed bedrock, late-stage acceleration.	Chamoli gives strong empirical support for progressive weakening.
3. Critical threshold / trigger	No single proximate trigger identified; intense rainfall and tectonic earthquake not supported.	Threshold failure after prolonged deformation; immediate timing mechanism debated.	Model must distinguish threshold state from trigger.
4. Rock-ice detachment	Recent reconstruction: ~103 Mm³ rock-ice mass failed near 5,190 m a.s.l., including ~12.6 Mm³ glacier ice (~12%); after ~30 s it struck and entrained a glacier tongue near 4,010 m, an initial vertical descent of ~1,180 m (Li et al., 2026).	~26.9 million m³ rock-ice wedge from Ronti Peak.	Both fit coupled rock-ice initiation. Nepal now has stronger quantitative source constraint, but direct source-volume comparison remains sensitive to reconstruction method and source composition.
5. Pathway amplification and flow bulking	After glacier impact, ~67 Mm³ was deposited in Chhochen Khola and ~36 Mm³ was remobilized into Lende Khola; progressive entrainment continued along an approximately 22-km upper-valley corridor (Li et al., 2026; Guo et al., 2026).	~1,800 m initial fall, confined Ronti Gad, strong erosion and entrainment.	Pathway properties strongly control final magnitude. Nepal's quantified deposition-remobilization partition, together with ~22 km of entrainment, shows that downstream hazard cannot be inferred from initial source volume alone.
6. Flow transformation and hydro-geomorphic coupling	Melt, external water and sediment incorporation; possible temporary river impoundment and release.	Rock-ice avalanche transformed to debris flow/hyperconcentrated flood; river and wet-substrate water important.	Hydrological availability and river/lake coupling enlarge hazard beyond source failure.
7. Exposure and disaster	Roads, bridges, hydropower, border facilities, settlements and ecosystems exposed along narrow valleys.	Two hydropower projects, workers and valley communities exposed.	Physical cascade becomes disaster through concentrated valley exposure.
8. Legacy risk	Altered channels, unstable sediment, barrier lakes and weakened slopes require continued monitoring.	Persistent channel/sediment reorganization; broader lessons for Himalayan preparedness.	Post-event landscape is a new, non-stationary hazard state.

5 Discussion

5.1 Comparative interpretation and explanatory performance of the CGDCM

The application of the CGDCM to Nepal 2026 and Chamoli 2021 showed that the two events shared strikingly similar higher-order process architecture while retaining important differences in source geometry, evidence quality, and hydrological context. Chamoli provides a stronger record of progressive pre-collapse deformation and subsequent thermomechanical flow transformation. Nepal provides strong new evidence that a transport corridor can amplify an event through progressive entrainment over approximately 22 km. Therefore, the two cases support complementary parts of the model rather than reproducing an identical causal sequence.

The independent, pre-event glacier reconstruction of Silwal et al. (2026) provides a useful test of CGDCM's explanatory consistency: multidecadal glacier thinning, retreat, fragmentation, and disconnection are compatible with the climate-conditioned susceptibility processes represented in Stages 1 and 2. However, demonstrating an event-specific causal role requires source-scale evidence on slope deformation, glacier–bedrock connectivity, thermal conditions, fracture development, and subsurface water pressures. CGDCM's contribution is to link established mechanisms into a coherent, testable process chain rather than to infer a unique proximate cause from regional glacier trends alone.

This comparative performance is consistent with the model's design as an integrative extension of the antecedent process chain and hazard-interaction science summarized in Section 3.3. The CGDCM does not require every event to activate every mechanism; rather, it provides a structured way to identify which domains are observed, which are physically plausible, which are weakly constrained, and where nonlinear amplification occurs. Table 3 summarizes the case-to-model mapping, and Table 1 distinguishes high-confidence observations from provisional or unresolved event-specific interpretations.

5.2 Climatic preconditioning, event attribution, and emerging institutional evidence

A central distinction in the CGDCM is between long-term climatic-cryospheric preconditioning and the proximate processes that determine the timing of the catastrophic failure. Anthropogenic warming does not need to function as an identifiable instantaneous trigger for climate change to be relevant to high mountain process chains. Instead, sustained warming can progressively modify glacier geometry and buttressing, permafrost integrity, rock-ice bonding, freeze-thaw regimes, meltwater production, drainage pathways, and stress distributions. These cumulative changes can move a coupled rock-ice slope progressively closer to a critical stability threshold. However, once failure occurs, the subsequent magnitude of the disaster may be governed increasingly by gravitational acceleration, fragmentation, entrainment, hydrological availability, topographic confinement, river interaction, and downstream exposure. Therefore, the CGDCM separates the climatic conditioning of susceptibility from the immediate trigger and the later amplification of the cascade.

The broader implications of planetary sustainability and accelerating Himalayan deglaciation for environmental integrity and Earth-system stability have been extensively examined by Upreti (1994, 2023), emphasizing the interconnectedness of cryospheric degradation, ecological vulnerability, and the sustainability of coupled human environment systems. Regional observations strongly support climatic preconditioning domain. In March 2026, the ICIMOD reported that glacier ice-loss rates across the Hindu Kush Himalaya have roughly doubled since 2000, with some monitored glaciers losing up to approximately 27 m of ice thickness since 1975 (ICIMOD, 2026a). The World Meteorological Organization (2025) reported that Asia is warming nearly twice as rapidly as the global average, whereas the IPCC identified glacier retreat, declining snow cover, permafrost thaw, and growing exposure of mountain infrastructure and downstream populations as major climate-sensitive risks (Adler et al., 2022; IPCC, 2022; Shaw et al., 2022). These regional trends strengthen the CGDCM preconditioning domain but do not, by themselves, establish the immediate trigger for a particular failure.

Recent quantitative evidence from Silwal et al. (2026) provides an important empirical foundation for the climatic–cryospheric preconditioning component of CGDCM. Their multitemporal reconstruction of glaciers in the Langtang catchment documented substantial glacier-area loss since the Little Ice Age, with the reported rate of recession during 2000–2023 approximately 1.5 times of that during 1964–2000. The study also recorded extensive thinning, fragmentation, separation, and disconnection, persistently negative glacier mass balance after 2000, rising equilibrium-line altitudes, and thinning across steep icefall zones. These observations establish a sustained evolution in glacier geometry, connectivity, and mass distribution in the wider Langtang catchment (Silwal et al., 2026).

From a cryosphere–geomechanical perspective, these changes are consistent with several interacting destabilization mechanisms represented in CGDCM. Glacier thinning and recession can diminish support to adjacent rock slopes, redistribute stresses, and expose previously ice-supported rock surfaces to thermal and hydrological changes. Fragmentation and disconnection can alter ice-flow continuity, while warming of ice-filled fractures and permafrost and greater meltwater access may reduce shear resistance, promote fracture propagation, and modify effective stress and basal sliding. Silwal et al. (2026) documented disconnection of the lower debris-covered tongue of Lirung Glacier from its upper ice body during the late twentieth century, illustrating such long-term reorganization. However, catchment-scale evidence neither establishes the mechanical condition of the August 2026 detachment surface nor identifies the proximate trigger. It instead strengthens the regional empirical basis and physical plausibility of the CGDCM sequence from climatic preconditioning through progressive weakening and eventual threshold failure.

Event-specific evidence requires the same causal discipline. Guo et al. (2026) found no intense rain trigger for the Nepal failure and did not identify a single direct trigger, while identifying meltwater availability, glacier motion, unusually warm conditions, and permafrost degradation as plausible weakening influences. For Chamoli, multi-year deformation, snow loading, permafrost degradation, rock fracture evolution, and glacier-rock interaction are plausible contributors; however, no single climatic variable uniquely fixes the time of collapse (Van Wyk de Vries et al., 2022; Zhou et al., 2021). Therefore, the scientifically defensible interpretation is that climate change can increase or redistribute susceptibility, even when the attribution of the precise failure time remains unresolved.

This distinction is increasingly reflected in Nepal's emerging institutional response to the 2026 catastrophe. The Ministry of Energy, Water Resources, and Irrigation initiated a multidisciplinary scientific investigation that treated the Rasuwa-Bhote Koshi event as a potential cascading disaster rather than a conventional rainfall-driven flood. The proposed investigation is expected to first reconstruct the source processes and event chronology, then evaluate interactions among glacier and rock-slope instability, mass movement, debris-flow transformation, river-system propagation, and downstream impacts, and only thereafter assess the possible contribution of anthropogenic climate change (Baahrakhari, 2026). This staged investigative strategy is scientifically important because it separates physical process reconstruction from climate attribution. Although the government initiative does not validate the CGDCM, its methodological logic independently converges with the framework's distinction between climatic preconditioning, cryosphere-geomechanical destabilization, threshold failure, and subsequent geomorphic hydrological amplification.

5.2.1 Exceptional antecedent thermal conditions

A preliminary meteorological reconstruction provides quantitative evidence of exceptional thermal conditions immediately preceding the 26 August 2026 rock–ice slope failure. Robert Rohde, chief scientist at Berkeley Earth, estimated air temperatures at the approximately 5,200-m failure site using the Copernicus ERA5 reanalysis dataset in combination with observations from 14 high-altitude meteorological stations located between 9 and 140 km from the collapsed glacier. The reconstruction indicated a mean temperature of approximately 5°C during 21–26 August, higher than any estimate for the corresponding six-day interval in more than 55 years of available records, during which temperatures had not previously exceeded 4°C. Rohde further estimated that the mean temperature for this six-day period at the failure site had increased by approximately 1.8°C since the mid-twentieth century. Without the additional warming associated with anthropogenic climate change, he calculated that a comparable temperature pattern “would probably occur only once in a few thousand years” (Agence France-Presse, 2026).

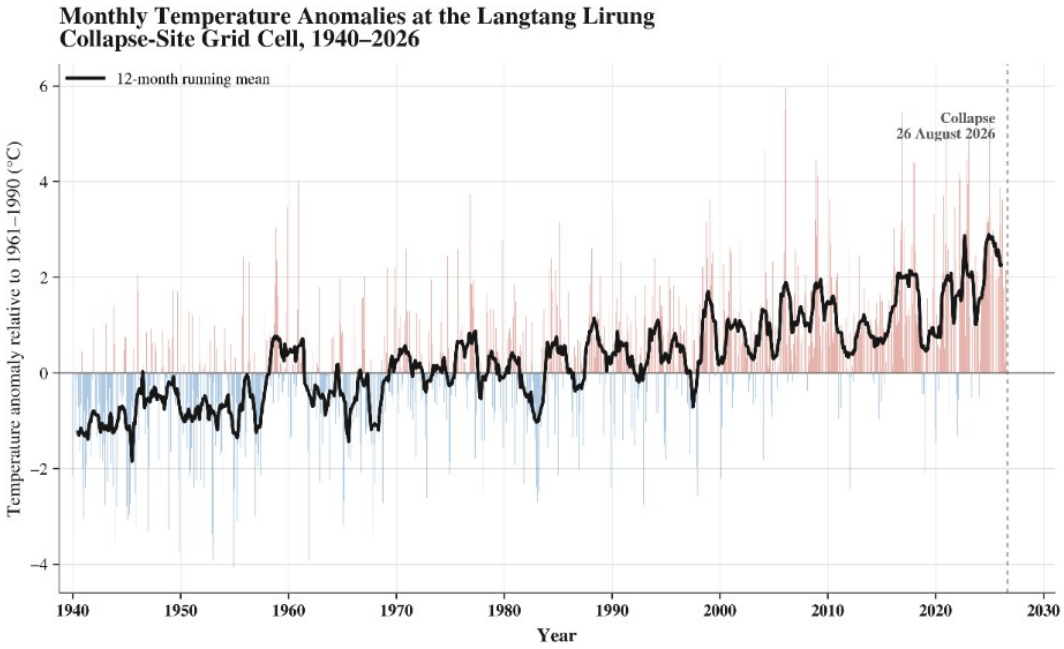


Figure 2. Monthly temperature anomalies at the collapse site relative to the 1961–1990 baseline, 1940–2026. Data from Hausfather (2026b); ERA5 reanalysis (Hersbach et al., 2020).

These findings support the interpretation of anomalous high-altitude warmth as a potentially important component of climatic preconditioning within the CGDCM. Nevertheless, because the reconstruction does not establish a direct causal relationship between the thermal anomaly and the slope failure, its principal evidentiary significance lies in documenting exceptionally strong antecedent thermal forcing. More definitive attribution will require process-based evidence demonstrating how elevated temperatures contributed to accelerated snow and ice melt, meltwater infiltration, permafrost degradation, fracture propagation, and the progressive weakening of the coupled rock–ice system.

A central scientific question is whether, and to what extent, climatic preconditioning shifts the probability distribution governing high-mountain glacier slope stability by progressively degrading the mechanical integrity of coupled rock–ice–permafrost systems. Establishing this relationship requires rigorous reconstruction of the event chronology and physical process chain, supported by multitemporal observations and process-based modeling capable of quantifying how glacier thinning and retreat, permafrost warming and degradation, enhanced meltwater infiltration, and evolving thermal and hydrological regimes modify stress distributions, fracture propagation, material strength, and, ultimately, the likelihood of threshold failure. It is in this context that the CGDCM offers a valuable integrative and analytical framework for systematically investigating, reconstructing, and interpreting the complete evolution of high-mountain cascading disasters from climatic preconditioning and progressive cryosphere–geomechanical destabilization through threshold failure, mass-movement transformation, geomorphic–hydrological amplification, and catastrophic downstream consequences.

5.3 Five testable propositions

P1: Climatic-cryospheric susceptibility. Long-term warming can alter glacier geometry, snow persistence, permafrost temperature, meltwater pathways, and rock-ice mechanical boundary conditions, thereby increasing or redistributing susceptibility without necessarily determining the precise time of failure. This proposition is strongly supported regionally but remains only moderately constrained for the timing of the two events.

P2: Progressive weakening may be observed. Where failure develops through cumulative deformation rather than instantaneous rupture, remote sensing, seismic, or geotechnical observations may reveal precursory motion or intermittent mass transfer. Chamoli provides strong support through multi-year displacement and late-stage acceleration, and Nepal provides provisional support through reported anomalous tremors before the main collapse.

P3: Pathway amplification decouples the impact from the source volume. Vertical relief, topographic confinement, entrainment potential, and hydrological availability can increase the mass, momentum, mobility, and destructive potential during runout; therefore, downstream magnitude cannot be inferred from the source volume alone. Nepal strongly supports this proposition through the Guo et al. (2026) reconstruction, and the 2016 Bhote Koshi and Sedongpu events provide independent process-level support (Gao et al., 2026; Liu et al., 2020).

P4 - Hydrological availability governs the flow regime transition. Frictional melting, snow/ice melt, wet sediment entrainment, river water, groundwater, and transient lake water can transform granular rock-ice avalanches into debris flows or hyperconcentrated floods. Chamoli thermomechanical modeling provides strong support, while Nepal is consistent with the proposition but still lacks an equivalent quantitative partitioning of water sources.

P5 - Disaster magnitude and persistence depend on exposure and legacy changes. The physical cascade becomes a societal catastrophe through interactions with people and infrastructure, whereas post-event sediment storage, altered channels, barrier lakes, and unstable slopes create a new risk state. Both Nepal and Chamoli support the exposure component, and the longer-term legacy component requires continued monitoring.

5.4 Transferability and falsifiability

The Nepal Bhote Koshi and India Chamoli comparison provides support for the transferability of the CGDCM, but it should not be described as a formal validation. Both cases were known during the model formulation and therefore functioned as comparative applications and consistency tests. Broader validation will require prospective use or application to additional events whose process sequences were not used to construct the framework. Transferability should therefore be evaluated at three distinct levels: (1) a transferable process architecture that organizes source, pathway, river, exposure, and legacy domains; (2) event-specific pathway activation and sequencing; and (3) site-specific quantitative thresholds that require calibration against local geomorphic, cryospheric, hydrological, and monitoring baselines.

The CGDCM is intended as a process-based framework for high-mountain cascading hazards in which climatic, cryospheric, geomechanical, geomorphic, and hydrological processes interact across source, pathway, and downstream domains. It is particularly applicable to cascades initiated within coupled rock-ice-glacier-permafrost terrain, but selected process domains may also apply to GLOFs, rainfall- or meltwater-triggered debris flows, landslide-dam failures, and tectonically triggered slope collapses where comparable entrainment, flow transformation, river interaction, downstream amplification, exposure, or legacy-risk processes occur. This bounded but flexible scope permits broader comparative use without treating the CGDCM as a universal model of all mountain hazards.

The model is falsifiable at the level of event-specific pathways. If future field and remote-sensing evidence from Nepal demonstrates negligible bedrock involvement, the initiation interpretation should shift toward an ice-dominated failure without invalidating downstream stages. If temporary river damming is not confirmed, the river interaction pathway should emphasize direct mass-water transfer rather than breach amplification. Conversely, verified pre-failure deformation, permafrost warming, meltwater pressurization, or repeatable seismic precursors would strengthen the weakening and threshold domains of the fault. Therefore, the CGDCM is a structured analytical framework, not a predetermined narrative. Therefore, transferability should be evaluated within the model's declared scope rather than by asking whether every Himalayan flood reproduces the complete CGDCM sequence. A convincing test is whether independent rock-ice cascade events can be mapped onto the defined domains without forcing absent mechanisms and whether the framework makes observations or process relationships that can subsequently be rejected. This bounded form of transferability is more scientifically useful than treating models as universal templates.

5.5 Regional analogue evidence and boundary testing

The wider Himalayan record shows that cascade amplification can occur under different initiating mechanisms. The 1981 Cirenmaco/Zhangzangbo GLOF demonstrated long-standing transboundary exposure in the Bhote Koshi corridor, whereas the 2016 Bhote Koshi event showed strong downstream amplification of a comparatively small lake release through sediment entrainment (Lamichhane et al., 2021; Liu et al., 2020). These cases support pathway amplification and exposure mechanisms without implying source-mechanical equivalence to Nepal 2026 or Chamoli 2021. The 2024 Thame event provides a contrasting boundary case in

which a rock avalanche struck a glacial lake, generated a displacement wave, and breached the lake (ICIMOD, 2025). The July 2025 Lhende-Rasuwagadhi flood, traced to transient supraglacial-lake drainage upstream of the Nepal-China border, likewise demonstrated rapid transboundary propagation with little useful local rainfall signal (Stimson Center, 2025, 2026). Such cases show that different cryosphere sources can converge on common downstream amplification and exposure processes.

Regional recurrence also has a predictive significance. Third Pole modeling projects an increasing GLOF risk under continued deglaciation, especially in transboundary mountain regions (Zheng et al., 2021), while Rather et al. (2026) emphasized the need for integrated monitoring and adaptation for rapidly changing Himalayan glacial-lake systems. The broader implication of the CGDCM is that hazard baselines are non-stationary and must be assessed dynamically across sources, pathways, and exposed systems.

5.6 Monitoring and predictive implications

The central operational implication is a shift from isolated hazard inventories to integrated source-pathway-river-exposure monitoring. Source areas require repeated observations of slope displacement, glacier motion, permafrost temperature, snowmelt conditions, fractures, and drainage anomalies. Transport corridors require mapping of relief, confinement, erodible sediments, water sources, and potential dam sites. Downstream systems require redundant seismic and hydrological detection, impact-based warnings, evacuation planning, and exposure analyses. Table 4 links the CGDCM domains to observable indicators and decision functions. Glacial lake inventories remain indispensable but are insufficient alone. GAPHAZ (2017) and regional inventories provide a foundation for surveillance; however, Nepal 2026 and Chamoli show that catastrophic cascades can begin on unstable rock-ice slopes without a large pre-existing lake. Therefore, monitoring should extend to hanging glaciers, permafrost-affected rock walls, slope deformation, unstable sediment stores, constricted channels, and potential transient dam sites (Rather et al., 2026; Adler et al., 2022; Bajracharya et al., 2020).

Quantitative operationalization follows a three-level logic. First, each CGDCM domain is linked to measurable variables in explicit units, including temperature and temperature trend, snow-cover duration, glacier mass balance and velocity, slope displacement and acceleration, source volume, flow velocity, river stage and discharge, entrainment ratio, and sediment-water characteristics. Second, event-specific empirical values are used as diagnostic examples: Chamoli exhibited more than 10 m of cumulative pre-collapse displacement over five years and late-stage velocities of approximately 0.5 m/day, whereas Nepal analyses reported post-detachment flow velocities of approximately 40-50 m/s (Van Wyk de Vries et al., 2022; Fan et al., 2022; GFZ German Research Centre for Geosciences, 2026). Third, operational alert thresholds should be calibrated to site-specific seasonal and long-term baselines and should emphasize acceleration, persistence, and convergence among independent signals. Because lithology, fracture geometry, glacier configuration, permafrost state, hydrology, and sensor resolution vary substantially among Himalayan slopes, these empirical examples should not be interpreted as universal failure thresholds.

Chamoli illustrates both the promise and the limits of precursor monitoring. Multi-year deformation was visible retrospectively, but the failure timing could not be predicted reliably from satellite data alone (Van Wyk de Vries et al., 2022). Nepal's precursor tremors are even less mature as warning signals. Therefore, operational systems should use probabilistic multi-sensor screening, including optical imagery, InSAR, GNSS, seismic, thermal, and hydrometeorological observations, rather than deterministic predictions from a single threshold variable (Ahmed et al., 2026).

Pathway monitoring is equally important because entrainment can govern the magnitude of a disaster after detachment. High-risk assessments should include unstable source volume, valley geometry, sediment availability, channel moisture, river discharge, damming potential, and exposed infrastructure. This source-pathway-exposure logic is the principal practical consequence of the CGDCM.

Table 4 Quantitative operationalization, testable observables, and decision implications of the CGDCM.

CGDCM component	Measurable indicators / metrics	Transition diagnostic / quantitative example	Operational implication
Climatic-cryospheric preconditioning	Air/ground temperature (°C; trend °C/decade); snow-cover duration (days/year); glacier area (% change), mass balance (m w.e./year) and velocity (m/year); permafrost/rock temperature (°C).	Persistent departures from local seasonal or decadal baselines indicate changing susceptibility; no direct event-timing threshold is implied.	Cryosphere observatories; dynamic susceptibility baselines and trend maps.
Cryosphere-geomechanical weakening	Crack opening (mm/day); InSAR/GNSS displacement (mm-m), velocity and acceleration; glacier-velocity anomaly (% or m/day); rock temperature; drainage or pore-pressure anomalies.	Acceleration or persistent deformation above site background. Chamoli example: >10 m displacement over five years and ~0.5 m/day shortly before failure; event-specific, not universal.	Multi-sensor source-area surveillance; site-calibrated anomaly thresholds.
Threshold / proximate trigger	Velocity acceleration (dV/dt); seismic/acoustic event rate, amplitude or energy, and spectral change; melt/rainfall intensity; drainage or pore-pressure change where instrumented.	Convergence of multiple anomalies and rapid acceleration relative to the local baseline is more diagnostic than any single cutoff.	Probabilistic multi-parameter alerts; escalation rules calibrated to local history.
Detachment and rapid acceleration	Seismic source parameters; optical change; source volume (m^3); vertical drop (m); trajectory; velocity (m/s).	Rapid mass-transfer signature and abrupt kinematic change. Nepal example: ~40-50 m/s after detachment; this is not a pre-failure threshold.	Automated mass-movement detection; rapid notification and downstream warning.
Pathway amplification and flow bulking	Relief/drop (m); confinement; erodible sediment volume (m^3); scour/deposition from DEM differencing; flow width/depth; entrainment ratio E = Vdownstream/Vsource or ΔV/Vsource.	E > 1 or increasing volume along runout indicates bulking; magnitude is event-specific. Nepal: progressive entrainment over an approximately 22-km upper-valley corridor.	Map amplification corridors and sediment stores, not source zones alone.
Hydrological availability and flow transformation	Water volume/fraction (% or m^3); wet-substrate moisture; ice/snow melt; sediment concentration (vol.% or mass%); density (kg/m^3); velocity/discharge; flow-regime indicators.	Transitions among granular avalanche, debris flow, debris flood, and hyperconcentrated flow should be inferred from measured or modelled water-sediment state; no universal concentration cutoff is prescribed.	Multiphase modelling; water-source partitioning; wet-sediment inventories.
River interaction	River stage (m), rate of rise (m/min), discharge (m^3/s); temporary-dam height/volume; impounded volume (m^3); breach timing; gauge loss; channel change.	Abrupt stage/discharge anomaly or verified impoundment/breach may mark renewed amplification; thresholds are reach-specific.	Barrier-lake detection; redundant gauges; breach scenarios and automated alarms.
Exposure and legacy risk	Exposed population/assets; infrastructure density and downtime; post-event DEM change; sediment storage (m^3); new-lake area/volume; repeat slope movement.	Impact scales with exposed receptors; persistent geomorphic change or renewed movement indicates a shifted post-event hazard baseline.	Risk-sensitive land use; recovery design; multi-season post-event monitoring.

7 Risk governance, infrastructure, and climate-equity implications

Both cases demonstrate the vulnerability of hydropower, roads, bridges, and human settlements concentrated within confined Himalayan valleys. Hazard governance should therefore require cryosphere-cascade screening in infrastructure design and environmental assessment, dynamic rather than static hazard maps, redundant warning systems, and multi-season post-event monitoring. The transboundary nature of the 2026 Nepal cascade additionally requires standing data-sharing protocols for glacier and slope motion, seismic signals, weather, river discharge, barrier lake formation, and satellite alerts. The Regional Cryosphere Strategy for the HKH provides a basis for harmonized monitoring and shared decision-making (Muhammad et al., 2026).

A practical policy architecture follows from this source-pathway-exposure logic and multi-hazard principles (Gill and Malamud, 2014; Kappes et al., 2012). Nepal should develop an integrated cryosphere-hazard

observation capability combining optical and radar remote sensing, InSAR, seismic monitoring, weather and river stations, glacier-velocity observations, cameras, drones, and anomaly detection. Transboundary basins require standing Nepal-China data protocols for slope, glacier, lake, seismic, meteorological, and discharge information, with downstream communication to India, where relevant (Lamichhane et al., 2021). Hazard maps should represent interacting cascades rather than isolated sectors such as floods, landslides, and GLOFs.

Infrastructure policy should move from historical design floods to lifetime multi-hazard risks. Hydropower, highways, bridges, border facilities, tourism nodes, and settlements in confined valleys should be screened for rock-ice avalanches, GLOFs, landslide dams, sediment waves, road isolation, and communication failures (Adler et al., 2022; IPCC, 2022; Lamichhane et al., 2021). Risk zoning should identify debris-flow and flood-corridor red zones, and reconstruction should avoid recreating the exposure. Hydropower design should incorporate emergency egress, redundant communications, upstream alarms, and rehearsed evacuation, reflecting a non-stationary cryosphere, rather than historical conditions alone (Shaw et al., 2022).

This risk-based approach should be paired with redundant last-mile warnings. Satellite and seismic detection must be rapidly connected to cell broadcasts, sirens, radios, satellite communications, mapped evacuation routes, and local drills. The July 2025 Rasuwagadhi event demonstrated the vulnerability of this transboundary corridor before the 2026 catastrophe (Stimson Center, 2025, 2026). Therefore, treating such events as institutional memories rather than isolated anomalies is central to adaptive governance.

For Nepal, these requirements also have a climate equity dimension. Nepal contributes only a very small share of global greenhouse gas emissions while facing high exposure to glacier loss, permafrost change, floods, and landslides (Government of Nepal, 2025; World Bank, 2022). International adaptation and Loss and Damage support for cryosphere observation, warning systems, and resilient reconstruction are therefore scientifically and ethically relevant, although the Paris Agreement does not establish liability or compensation through Article 8 (UNFCCC, 2016). A concise mountain-risk case can appropriately inform Nepal's COP31 diplomacy.

5.8 Limitations and research priorities

The principal limitation of this study is the temporal proximity of the Nepal event. Guo et al. (2026) provided an important *peer-reviewed* reconstruction; however, complete field-based geotechnical, geomorphological, hydrological, and climate-attribution studies remain unavailable. Source composition, the relative timing of bedrock and glacier detachment, the volume of internally generated versus externally acquired water, the magnitude of entrainment, and the role of transient impoundment require further investigation. Chamoli is better constrained but retains uncertainties in heat transfer physics, initial water content, substrate saturation, and the hydrometeorological state of the entrainment layers (Munch et al., 2024). The quantitative values reported in this paper and summarized in Table 4 are therefore used as measurement examples or event-specific diagnostics, not as universal Himalayan failure thresholds. The recently initiated Government of Nepal multidisciplinary investigation is therefore particularly timely and may provide the critical field, geomorphic, hydrological, and climate-attribution evidence needed to evaluate these unresolved aspects of the event (Baahrakhari, 2026). The historical and regional cases used here also have a specific methodological limitation: they are not assumed to share the same source mechanics as the Nepal 2026 or Chamoli 2021. Their role is to test individual mechanisms and model boundaries, especially entrainment, lake/river interaction, transboundary propagation, infrastructure exposure, and legacy risk, rather than inflating the number of apparent CGDCM applications.

These unresolved questions, together with the newly initiated national investigation, define several priority research areas. These include high-resolution comparisons of pre- and post-event Digital Elevation Models (DEMs) to quantify terrain change, erosion, deposition, and displaced material volumes; seismic wave form inversion; thermo-hydro-mechanical modeling of rock-ice interfaces; multiphase entrainment and runout modeling; field-based sediment budgets; reconstruction of transient dams and water sources; and long-term permafrost and rock temperature monitoring. Climate-attribution studies should focus on how climatic warming alters the probability of destabilizing preconditions rather than simplistic single-event causation. Comparative application to additional well-documented events, including Sedongpu and future rock-ice avalanches, will be necessary before the CGDCM can be regarded as a broadly validated predictive framework.

6 Conclusions

The August 2026 Bhote Koshi-Trishuli catastrophe and the February 2021 India Chamoli disaster cannot be adequately understood using single-hazard labels. Nepal catastrophe was not a conventional local rainfall flood,

and Chamoli was not a glacial-lake outburst. Both began with instability in high-altitude rock-ice systems and evolved through gravitational, geomorphic, and hydrological transformations into destructive downstream flows.

The CGDCM is explicitly rooted in prior multi-hazard interactions, glacier-permafrost hazards, high-mountain process chains, rock-ice mechanics, and multiphase-flow research. Its contribution is not the invention of the individual mechanisms but their integration into a bounded causal architecture linking climatic-cryospheric preconditioning, progressive cryosphere-geomechanical weakening, critical-threshold crossing, detachment, pathway amplification, hydro-geomorphic transformation, exposure, infrastructure cascade and legacy risk. Within this architecture, climatic warming is treated principally as a cumulative conditioner of susceptibility, capable of altering glacier support, permafrost integrity, rock-ice bonding, meltwater pathways, and slope stability, rather than as an assumed instantaneous trigger of failure. Within this architecture, climate change is treated principally as a conditioning influence on susceptibility rather than as a necessary instantaneous trigger. Sustained warming can progressively alter glacier support, permafrost integrity, rock-ice bonding, meltwater pathways, and slope stability, moving a coupled mountain system toward a critical threshold without uniquely determining the timing of failure. This distinction provides a more defensible basis for climate attribution in complex cascading disasters and is consistent with Nepal's newly initiated staged scientific investigation of the 2026 event (Baahrakhari, 2026). Independently documented multidecadal glacier thinning, fragmentation, and disconnection in the Langtang catchment provide regional empirical support for the climate-conditioned susceptibility mechanisms represented in CGDCM, although event-specific causal attribution remains an important subject for further investigation (Silwal et al., 2026).

The comparative cases support different aspects of this architecture. Chamoli provides strong empirical evidence for progressive pre-collapse deformation and quantitative thermomechanical evidence of water-mediated flow-regime transformation. The Nepal reconstruction quantitatively corroborates the CGDCM by showing that a ~103 Mm^3 source failure was substantially redistributed and remobilized downstream, demonstrating that cascade evolution, not source volume alone, governs final disaster magnitude. Newly available evidence from Nepal provides especially strong support for the proposition that progressive entrainment and hydrological availability along the transport corridor can determine downstream intensity independently of initial source volume. Historical Bhote Koshi, Thame, Sedongpu, and other regional examples further demonstrate that similar amplification mechanisms can recur under different source processes while defining the boundaries of the model.

Five propositions make the framework testable: climate-conditioned susceptibility should evolve independently of the exact trigger timing; progressive weakening may produce observable precursors; pathway amplification can decouple the impact from the source volume; hydrological availability can control flow-regime transition; and disaster magnitude and persistence depend on exposure and post-event landscape change. These propositions can be evaluated using remote sensing, geotechnical and seismic observations, multiphase numerical modeling, sediment budgets, and prospective event comparisons. Their operationalization should combine measurable physical variables with site-calibrated baselines and multivariate anomaly detection rather than universal numerical failure cutoffs.

Operationally, the CGDCM implies that risk management must monitor the complete source-pathway-river-exposure system rather than only glacial lakes or downstream river levels. Dynamic cryosphere observation, multi-hazard mapping, pathway and sediment inventories, redundant early warning, cryosphere-sensitive infrastructure design, transboundary data sharing, and multi-season legacy-risk monitoring are therefore integral to anticipatory risk governance in the Himalayan region. A central scientific and risk-governance question is not only where and under what conditions a high-altitude glacier rock–ice mass may fail, but also how topographic confinement, sediment entrainment, water availability, and downstream channel interactions may transform and amplify the initial failure and how society can interrupt its progression from cascading hazard to catastrophe through monitoring, early warning, risk-sensitive land-use planning, and disaster preparedness.

Acknowledgements

The author acknowledges the scientists, hydrological services, remote-sensing teams, geophysical agencies, and research institutions that released rapid observations and interpretations used in this synthesis. Their data sharing made comparative analysis possible while the August 2026 Nepal catastrophe was still under active investigation. The author is solely responsible for the formulation and interpretation of the proposed CGDCM.

References

Adler, C., Wester, P., Bhatt, I., Huggel, C., Insarov, G. E., Morecroft, M. D., Muccione, V., Prakash, A., 2022. Cross-Chapter Paper 5: Mountains. In: Pörtner, H.-O., Roberts, D. C., Tignor, M., et al., eds., Climate Change 2022: Impacts, Adaptation and Vulnerability. Cambridge University Press, Cambridge, 2273-2318. https://doi.org/10.1017/9781009325844.022

Agence France-Presse. (2026, September 8). *Nepal glacier saw exceptional heat before collapse caused deadly floods: Researcher*. Phys.org. https://phys.org/news/2026-09-nepal-glacier-exceptional-collapse-deadly.html

Ahmed, R., Bhardwaj, A., Sam, L., et al., 2026. Ice-Rock Avalanches in a Warming Himalaya Indicate Pathways toward Effective Preparedness. Communications Earth & Environment, 7: 217. https://doi.org/10.1038/s43247-02603352-y

Alangadan, A., Sattar, A., 2026. Permafrost Distribution, Degradation, and Potential Mass Movement Cascades in the Western Himalaya Using Machine Learning and Numerical Models. npj Natural Hazards, 3: 49. https://doi.org/10.1038/s44304-026-00217-4

Azam, M. F., 2026. HKH Glacier Outlook 2026: Understanding Change through 50 Years of Field Observation. International Centre for Integrated Mountain Development, Kathmandu. https://doi.org/10.53055/ICIMOD.1123

Bajracharya, S. R., Maharjan, S. B., Shrestha, F., Sherpa, T. C., Wagle, N., Shrestha, A. B., 2020. Inventory of Glacial Lakes and Identification of Potentially Dangerous Glacial Lakes in the Koshi, Gandaki, and Karnali River Basins of Nepal, the Tibet Autonomous Region of China, and India. ICIMOD and UNDP, Kathmandu. https://doi.org/10.53055/ICIMOD.773

Baahrakhari, 2026. Scientific Investigation of the Rasuwa Flood to Be Conducted by a Team Including International Experts. Baahrakhari, Kathmandu, September 13, 2026. [In Nepali]. https://baahrakhari.com/detail/501273

Fan, X. M., Yunus, A. P., Yang, Y. H., et al., 2022. Imminent Threat of Rock-Ice Avalanches in High Mountain Asia. Science of the Total Environment, 836: 155380. https://doi.org/10.1016/j.scitotenv.2022.155380

Fischer, L., Purves, R. S., Huggel, C., et al., 2012. On the Influence of Topographic, Geological and Cryospheric Factors on Rock Avalanches and Rockfalls in High-Mountain Areas. Natural Hazards and Earth System Sciences, 12: 241-254. https://doi.org/10.5194/nhess-12-241-2012

Gao, Y., Zhuang, Y., Li, B., Dash, R. K., Li, J., Bartelt, P., Yin, Y., 2026. Entrainment-Driven Transition from Avalanche to Debris Flow: Insights from the 2018 Sedongpu Event. Journal of Geophysical Research: Earth Surface, 131: e2025JF008750. https://doi.org/10.1029/2025JF008750

GAPHAZ, 2017. Assessment of Glacier and Permafrost Hazards in Mountain Regions: Technical Guidance Document. Prepared by Allen, S., Frey, H., Huggel, C., et al. Standing Group on Glacier and Permafrost Hazards in Mountains (GAPHAZ), Zurich, Switzerland/Lima, Peru, 72 p. https://doi.org/10.13140/RG.2.2.26332.90245

GFZ German Research Centre for Geosciences, 2026. Extreme Flooding in China and Nepal: What We Know So Far. GFZ, Potsdam, August 27, 2026.

Gill, J. C., Malamud, B. D., 2014. Reviewing and Visualizing the Interactions of Natural Hazards. Reviews of Geophysics, 52(4): 680-722. https://doi.org/10.1002/2013RG000445

Government of Nepal, 2025. Nationally Determined Contribution (NDC) 3.0. Ministry of Forests and Environment, Kathmandu.

Gruber, S., Fleiner, R., Guegan, E., et al., 2017. Inferring Permafrost and Permafrost Thaw in the Mountains of the Hindu Kush Himalaya Region. The Cryosphere, 11: 81-99. https://doi.org/10.5194/tc-11-81-2017

Guo, L., Xu, J., Wang, Y., Hu, Y., Peng, F., et al., 2026. Progressive Entrainment Transformed a High-Elevation Ice-Rock Avalanche in Nepal into the 26 August Debris Flow in Gyirong, Xizang. Chinese Science Bulletin, online first. https://doi.org/10.1360/CSB-2026-1255

Haeberli, W., Schaub, Y., Huggel, C., 2017. Increasing Risks Related to Landslides from Degrading Permafrost into New Lakes in De-Glaciating Mountain Ranges. Geomorphology, 293: 405-417. https://doi.org/10.1016/j.geomorph.2016.02.009

Hausfather, Z. (2026a, August 28). *What we can and cannot say about climate change and the Nepal disaster*. The Climate Brink. https://www.theclimatebrink.com/p/what-we-can-and-cannot-say-about

Hausfather, Z. (2026b). *Langtang-glacier-collapse: Data and analysis code for the Langtang Lirung collapse* [Data set and computer software]. GitHub. https://github.com/hausfath/langtang-glacier-collapse

Hersbach, H., Bell, B., Berrisford, P., Hirahara, S., Horányi, A., Muñoz-Sabater, J., Nicolas, J., Peubey, C., Radu, R., Schepers, D., Simmons, A., Soci, C., Abdalla, S., Abellan, X., Balsamo, G., Bechtold, P.,

Biavati, G., Bidlot, J., Bonavita, M., … Thépaut, J.-N. (2020). The ERA5 global reanalysis. *Quarterly Journal of the Royal Meteorological Society, 146*(730), 1999–2049. https://doi.org/10.1002/qj.3803

Intergovernmental Panel on Climate Change (IPCC), 2022. Climate Change 2022: Impacts, Adaptation and Vulnerability. Cambridge University Press, Cambridge. https://doi.org/10.1017/9781009325844

International Centre for Integrated Mountain Development, 2023. Water, Ice, Society, and Ecosystems in the Hindu Kush Himalaya: An Outlook. ICIMOD, Kathmandu. https://doi.org/10.53055/ICIMOD.1028

International Centre for Integrated Mountain Development, 2025. Everest Region a Hotspot of Cryosphere-Linked Hazards, ICIMOD's New Study on Nepal's 2024 Thame Flood Confirms. ICIMOD, Kathmandu, October 14, 2025.

International Centre for Integrated Mountain Development, 2026a. Hindu Kush Himalaya Glaciers Losing Ice at Double the Rate Since 2000, New ICIMOD Reports Confirm. ICIMOD, Kathmandu, March 18, 2026.

International Centre for Integrated Mountain Development, 2026b. Kyirong-Rasuwa Flood 2026: Nepal-China Cryosphere Risk. ICIMOD, Kathmandu, August 26, 2026.

Kappes, M. S., Keiler, M., von Elverfeldt, K., Glade, T., 2012. Challenges of Analyzing Multi-Hazard Risk: A Review. Natural Hazards, 64(2): 1925-1958. https://doi.org/10.1007/s11069-012-0294-2

Krautblatter, M., Funk, D., Günzel, F. K., 2013. Why Permafrost Rocks Become Unstable: A Rock-Ice-Mechanical Model in Time and Space. Earth Surface Processes and Landforms, 38(8): 876-887. https://doi.org/10.1002/esp.3374

Lamichhane, S., Aryal, K. R., Talchabhadel, R., Thapa, B. R., Adhikari, R., Khanal, A., Pandey, V. P., Gautam, D., 2021. Assessing the Prospects of Transboundary Multihazard Dynamics: The Case of Bhotekoshi-Sunkoshi Watershed in Sino-Nepal Border Region. Sustainability, 13(7): 3670. https://doi.org/10.3390/su13073670

Li, H., Li, P., Hu, K., Liu, J., Liu, S., Kang, S., Su, P., You, Y., 2026. The 26 August 2026 Chhochen Khola Ice Rock Avalanche-Debris Flow Cascade on the Nepal-China Border: Dynamics, Numerical Computation, and Causes. Journal of Mountain Science. https://doi.org/10.1007/s11629-026-1482-y

Li, Y., Fan, X. M., Ni, T., Wang, W., Wang, Q., Zhang, X., Pan, Q., 2025. Centrifuge Model Investigation on the Initiation Mechanisms of Rock-Ice Slide: Insights from the Yigong Landslide and Chamoli Rock-Ice Avalanche. Engineering Geology, 354: 108192. https://doi.org/10.1016/j.enggeo.2025.108192

Liu, M., Chen, N., Zhang, Y., Deng, M., 2020. Glacial Lake Inventory and Lake Outburst Flood/Debris Flow Hazard Assessment after the Gorkha Earthquake in the Bhote Koshi Basin. Water, 12(2): 464. https://doi.org/10.3390/w12020464

Maharjan, S. B., Sherpa, T. C., 2026. Changing Dynamics of Glaciers in the Hindu Kush Himalayan Region from 1990 to 2020. International Centre for Integrated Mountain Development, Kathmandu. https://doi.org/10.53055/ICIMOD.1122

Mamot, P., Weber, S., Eppinger, S., et al., 2021. A Temperature-Dependent Mechanical Model to Assess the Stability of Degrading Permafrost Rock Slopes. Earth Surface Dynamics, 9: 1125-1151. https://doi.org/10.5194/esurf-9-1125-2021

Mani, P., Allen, S., Evans, S. G., et al., 2023. Geomorphic Process Chains in High-Mountain Regions-A Review and Classification Approach for Natural Hazards Assessment. Reviews of Geophysics, 61(4): e2022RG000791. https://doi.org/10.1029/2022RG000791

Maurer, J. M., Schaefer, J. M., Rupper, S., Corley, A., 2019. Acceleration of Ice Loss across the Himalayas over the Past 40 Years. Science Advances, 5(6): eaav7266. https://doi.org/10.1126/sciadv.aav7266

Mergili, M., Pfeffer, H., Kellerer-Pirklbauer, A., Zangerl, C., Pudasaini, S. P., 2025. r.avaflow v4, a Multi-Purpose Landslide Simulation Framework. Geoscientific Model Development, 18: 9879-9896. https://doi.org/10.5194/gmd-18-9879-2025

Muhammad, S., Azam, M. F., Jackson, M., Zhang, Q., 2026. Regional Cryosphere Strategy for the Hindu Kush Himalaya. Journal of Mountain Science, 23: 2983-2991. https://doi.org/10.1007/s11629-025-0357-y

Munch, J., Zhuang, Y., Dash, R. K., Bartelt, P., 2024. Dynamic Thermomechanical Modeling of Rock-Ice Avalanches: Understanding Flow Transitions, Water Dynamics, and Uncertainties. Journal of Geophysical Research: Earth Surface, 129: e2024JF007805. https://doi.org/10.1029/2024JF007805

OnlineKhabar, 2026a. The Bhote Koshi Flood Was Not Caused by Rainfall. OnlineKhabar, August 26, 2026.

OnlineKhabar, 2026b. Technical Report Details Bhotekoshi Flood's Journey from Tibet to Devghat. OnlineKhabar, August 27, 2026.

Pudasaini, S. P., Mergili, M., 2019. A Multi-Phase Mass Flow Model. Journal of Geophysical Research: Earth Surface, 124: 2920-2942. https://doi.org/10.1029/2019JF005204

Rather, A. F., Ahmed, R., Shamim, T., Farooq, A., Mir, R. A., Wani, O., Gulzar, S. H., Ahmed, P., 2026. Glacial Lakes and GLOFs in a Warming Himalaya-Karakoram Region: Current Understanding, Challenges, and the Way Forward. npj Natural Hazards, 3: 7. https://doi.org/10.1038/s44304-026-00168-w

Richter, H., Parvaiz, A., 2026. How Scientists Unraveled the Cause of the Devastating Flood in Tibet and Nepal. Science, August 28, 2026.

Shaw, R., Luo, Y., Cheong, T. S., Abdul Halim, S., Chaturvedi, S., Hashizume, M., Insarov, G. E., Ishikawa, Y., Jafari, M., Kitoh, A., Pulhin, J., Singh, C., Vasant, K., Zhang, Z., 2022. Asia. In: Pörtner, H.-O., Roberts, D. C., Tignor, M., et al., eds., Climate Change 2022: Impacts, Adaptation and Vulnerability. Cambridge University Press, Cambridge.

Shugar, D. H., Jacquemart, M., Shean, D., et al., 2021. A Massive Rock and Ice Avalanche Caused the 2021 Disaster at Chamoli, Indian Himalaya. Science, 373(6552): 300-306. https://doi.org/10.1126/science.abh4455

Silwal, G., Davies, B., Carr, J. R., et al., 2026. Glacier Changes in Langtang Catchment, Central Nepalese Himalaya from the Little Ice Age (~1815 CE) to 2023 CE. Global and Planetary Change, 264: 105555. https://doi.org/10.1016/j.gloplacha.2026.105555

Stimson Center, 2025. Investigating an Emerging Climate Hazard: Transboundary Glacial Floods on the China-Nepal Border. Stimson Center, Washington, DC.

Stimson Center, 2026. Climate Risks to Nepal's Energy Transition: Loss and Damage from a Glacial Lake Disaster Disrupting the Trans-Himalayan EV Supply Chain. Stimson Center, Washington, DC.

U.S. Geological Survey, 2026. 2026 Nepal Debris Avalanche and Flash Flood. U.S. Geological Survey, August 27, 2026.

United Nations Framework Convention on Climate Change, 2016. Decision 1/CP.21: Adoption of the Paris Agreement. UNFCCC, Bonn.

Upreti, G., 2023. *Ecosociocentrism: The Earth First Paradigm for Sustainable Living.* Springer Nature Switzerland, Cham. https://doi.org/10.1007/978-3-031-41754-2

Upreti, G., 1994. *Environmental Conservation and Sustainable Development Require a New Development Approach. Journal of Environmental Conservation, Vol. 21(18-29), 1994*.

Van Wyk de Vries, M., Bhushan, S., Jacquemart, M., et al., 2022. Pre-Collapse Motion of the February 2021 Chamoli Rock-Ice Avalanche, Indian Himalaya. Natural Hazards and Earth System Sciences, 22: 3309-3327. https://doi.org/10.5194/nhess-22-3309-2022

Wang, Q., Zhang, Y., Peng, X., Ma, L., Li, C., Xiao, Y., Yu, P., Cheng, Q., 2025. Development of a Coupled DDA-SPH Method and Its Application to Fracture and Dynamic Simulation of Ice-Rock Interaction. Engineering Geology, 357: 108310. https://doi.org/10.1016/j.enggeo.2025.108310

World Bank, 2022. Nepal Country Climate and Development Report: Towards a Green, Resilient, and Inclusive Development. World Bank, Washington, DC.

World Meteorological Organization, 2025. State of the Climate in Asia 2024. World Meteorological Organization, Geneva.

Yin, Y., Xing, A., Zhuang, Y., Wang, Q., 2025. Destructive Potential of the Chamoli Rock-Ice Avalanche-Induced Air Blasts. Journal of Rock Mechanics and Geotechnical Engineering, 17(10): 6111-6119. https://doi.org/10.1016/j.jrmge.2024.11.053

Zheng, G., Allen, S. K., Bao, A., Ballesteros-Cánovas, J. A., Huss, M., Zhang, G., Li, J., Yuan, Y., Jiang, L., Yu, T., Chen, W., Stoffel, M., 2021. Increasing Risk of Glacial Lake Outburst Floods from Future Third Pole Deglaciation. Nature Climate Change, 11: 411-417. https://doi.org/10.1038/s41558-021-01028-3

Zhou, Y., Li, X., Zheng, D., Li, Z., An, B., Wang, Y., Jiang, D., Su, J., Cao, B., 2021. The Joint Driving Effects of Climate and Weather Changes Caused the Chamoli Glacier-Rock Avalanche in the High Altitudes of the India

Himalaya. Science China Earth Sciences, 64(11): 1909-1921. https://doi.org/10.1007/s11430-021-9844-0

About the author

Gopi Upreti
Emeritus Professor, Institute of Agriculture and Animal Sciences (IAAS), Tribhuvan University, Nepal.
STAR Scholar Network Environment and Climate Policy Laureate

Email: goupreti@gmail.com

Gopi Upreti is an *Emeritus Professor* at Tribhuvan University (IAAS) with more than three decades of distinguished services in teaching, research, and academic leadership. His foundational academic credentials include BSc. Ag (Hons). from Punjab Agriculture University (1978), MS in Agriculture, University of Hawaii (1983), MS in Environmental Resource Management, UH (1990), and doctoral fellow in Agriculture from 1988 to 1992 at University of Hawaii. He has held senior academic and institutional roles, including Chief Commissioner of Nepal Agriculture Research Council (NARC) and Strategic Policy Advisor to the Environmental Protection Council (EPC), Government of Nepal. His scholarship spans regenerative agriculture, environmental and earth science, and sustainable development, and includes dozens of peer-reviewed journal articles, review papers, books, and book chapters.

Prof. Upreti received the coveted *Best Paper Award* from the Switzerland based International Foundation of Environmental Conservation for his seminal paper *"Environmental Conservation and Sustainable Development Require a New Development Approach,"* featured in the *Journal of Environmental Conservation, Vol. 21(18-29), 1994*. He is the author of groundbreaking book *Ecosociocentrism: The Earth First Paradigm for Sustainable Living, published by* Springer Nature Switzerland AG, 2023. His environmental philosophical Epic *"From Ruin to Renewal"* was published by Global STAR Scholar Network in 2026.

He lives in Fairfax, Virginia, United States of America (USA).